ACCOUNTS
of chemical research

Molecular Electronic Devices Based on Single-Walled Carbon Nanotube Electrodes

ALINA K. FELDMAN,[†] MICHAEL L. STEIGERWALD,[†]
XUEFENG GUO,[*,‡] AND COLIN NUCKOLLS[*,†]

[†]*Department of Chemistry and the Columbia University Center for Electronics of Molecular Nanostructures, Columbia University, New York, New York 10027,* [‡]*Centre for Nanochemistry (CNC), Beijing National Laboratory for Molecular Sciences (BNLMS), State Key Laboratory for Structural Chemistry of Unstable and Stable Species, College of Chemistry and Molecular Engineering, Peking University, Beijing 100871, P. R. China*

RECEIVED ON JANUARY 28, 2008

CONSPECTUS

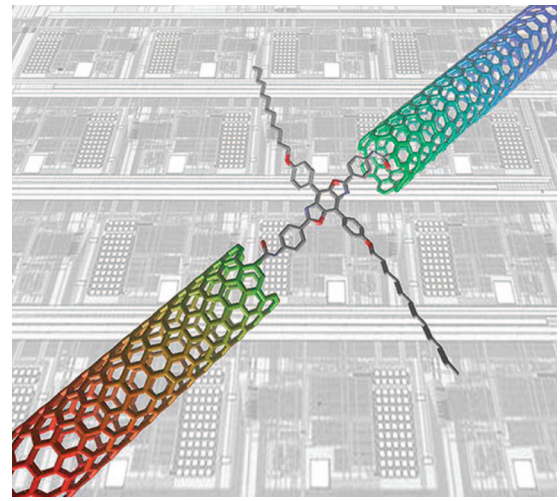

As the top-down fabrication techniques for silicon-based electronic materials have reached the scale of molecular lengths, researchers have been investigating nanostructured materials to build electronics from individual molecules. Researchers have directed extensive experimental and theoretical efforts toward building functional optoelectronic devices using individual organic molecules and fabricating metal−molecule junctions. Although this method has many advantages, its limitations lead to large disagreement between experimental and theoretical results.

This Account describes a new method to create molecular electronic devices, covalently bridging a gap in a single-walled carbon nanotube (SWNT) with an electrically functional molecule. First, we introduce a molecular-scale gap into a nanotube by precise oxidative cutting through a lithographic mask. Now functionalized with carboxylic acids, the ends of the cleaved carbon nanotubes are reconnected with conjugated diamines to give robust diamides. The molecular electronic devices prepared in this fashion can withstand and respond to large environmental changes based on the functional groups in the molecules. For example, with oligoanilines as the molecular bridge, the conductance of the device is sensitive to pH. Similarly, using diarylethylenes as the bridge provides devices that can reversibly switch between conjugated and nonconjugated states.

The molecular bridge can perform the dual task of carrying electrical current and sensing/recognition through biological events such as protein/substrate binding and DNA hybridization. The devices based on DNA can measure the difference in electrical properties of complementary and mismatched strands. A well-matched duplex DNA 15-mer in the gap exhibits a 300-fold lower resistance than a duplex with a GT or CA mismatch. This system provides an ultrasensitive way to detect single-nucleotide polymorphisms at the individual molecule level. Restriction enzymes can cleave certain cDNA strands assembled between the SWNT electrodes; therefore, these strands maintain their native conformation when bridging the ends of the SWNTs.

This methodology for creating novel molecular circuits forges both literal and figurative connections between chemistry, physics, materials science, and biology and promises a new generation of integrated multifunctional sensors and devices.

Published on the Web 09/18/2008 www.pubs.acs.org/acr
10.1021/ar8000266 CCC: $40.75

Introduction

This Account details a new method to create molecular electronic devices, covalently bridging a gap in a single-walled carbon nanotube (SWNT) with an electrically functional molecule. The top-down fabrication techniques developed for silicon-based electronic materials have reached molecular length scales. Using these tools with nanostructured materials, themselves created through bottom-up chemical methods, provides paths to new materials and devices. We grow individual SWNTs that span metal electrodes and lithographically excise a section of the nanotube, producing gaps of 1−10 nm. We detail below bridging these gaps with molecules and the properties of the devices that result.

There has been extensive experimental and theoretical effort directed toward creating functional optoelectronic devices using individual organic molecules.[1−7] Individual organic molecules have both ultrasmall dimensions and an overwhelming degree of diversity and functionality, with essentially full control over molecular design through chemical synthesis. Multiple approaches are being explored for metal−molecule−metal junction fabrication,[8−12] the most common being insertion of α,ω-dithiols between gold electrodes (Figure 1).[7,12−16] Although this method has many advantages, it suffers from some limitations: thiols are susceptible to air oxidation;[17] gold electrode fabrication is difficult; precise control over contact geometry is challenging; it is difficult to control the exact number of molecular bridges. As a result, experimental charge-transport data gives broad ranges of values for molecular conductance, and large disagreement exists between experimental and theoretical results.[11,12,18,19]

An improved strategy would create a well-defined contact between the electrode and the molecule, would have a limited number of binding sites, and would be intrinsically molecular. Since their discovery,[20] carbon nanotubes have been regarded as an exceptional material.[21,22] Single-walled carbon nanotubes (SWNTs) have elementary chemical composition and bonding but exhibit perhaps the highest degree of diversity among nanomaterials.[23−25] SWNTs are one-dimensional (1D) ballistic nanowires that are intrinsically molecular, they can be processed, and their π-bonding affords useful electrical behavior. SWNTs can be either metallic or semiconducting, which gives rise to unlimited electrical versatility. Were one to connect different SWNTs with different "molecular solders", the various energy alignments between the tubes and the bridging molecules would give a variety of physical behaviors. The important distinction between the SWNTs and ordinary metal contacts is that SWNTs are molecularly sized in their width, infinitely long, and functional on their ends (but not their sides). Thus, SWNTs are ideal contacts for flexible and modular single-molecule devices.

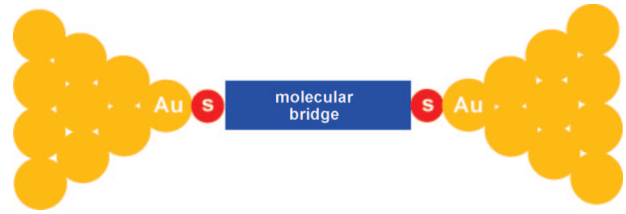

FIGURE 1. A single molecule between two gold contacts.

Preparation of SWNTs as Point Contacts

We make SWNT electrodes by cutting the nanotubes by spatially resolved oxidation, leaving two ends separated by ≤10 nm.[26] Our idea was based on work by Dai and co-workers where carbon nanotubes were cut and used as contacts for organic field effect transistors (OFETs).[27] Our strongly oxidizing conditions produce tube ends that are capped with carboxylic acids.[28] SWNTs are grown by chemical vapor deposition (CVD) on silicon wafers to yield individual ∼1−2 nm diameter nanotubes.[29] This method is illustrated in Figure 2. First, a <10 nm window is opened in a spin-cast masking layer of poly(methyl methacrylate) (PMMA) by electron-beam lithography. Oxygen plasma ion etching cuts the nanotubes through the open window. The PMMA is removed, leaving the carboxylate-functionalized SWNT point contacts. The gap is located and imaged with atomic force microscopy (AFM, Figure 2C).

The degree of cutting (and therefore the gap size) can be controlled by varying the etching time. While longer etch times give higher yields of cut tubes, they also give gaps that are more difficult to bridge. Under optimized conditions, ∼20−25% of the tubes are completely cut. As we imply in Figure 2, we deposit the SWNTs on SiO_2 on doped Si, and we make electrical contact to the remote ends of the tubes via thermal evaporation of Au. When the gap is bridged by a conductive molecule, the assembly acts as a wire or a field-effect transistor, depending on the details of the constituent parts.

Covalently Bridging Gaps in SWNTs with Molecular Wires

A molecular bridge with the desired functionality is attached to the carboxylates at the tube ends.[26] The "molecular solders" are diamines; these are attached by immersing the SWNT devices in a pyridine solution containing the

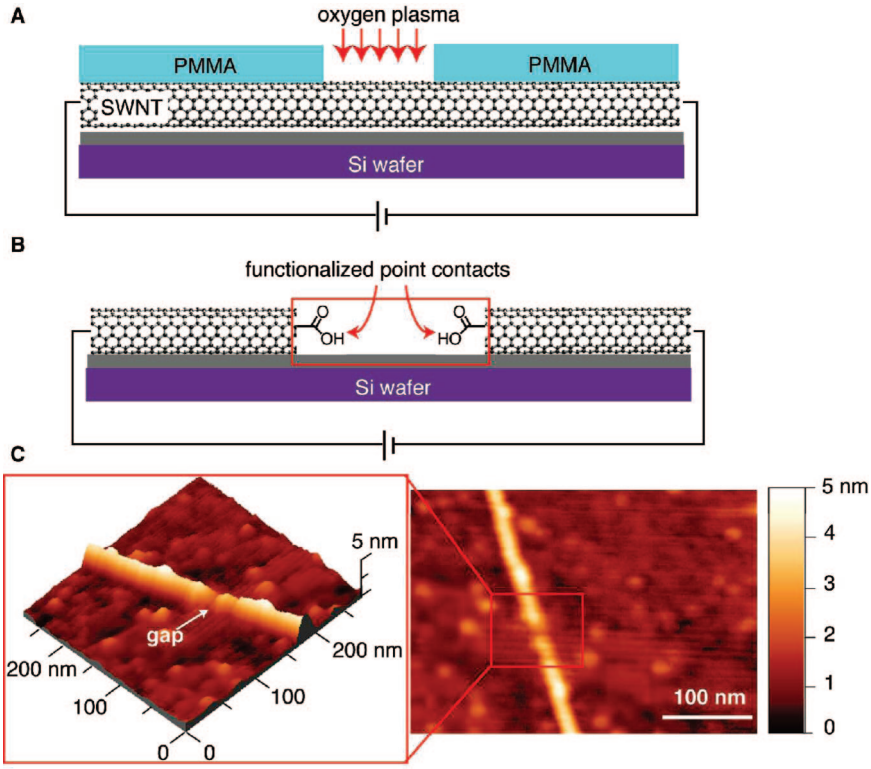

FIGURE 2. (A) Oxygen plasma introduced through a defined PMMA window achieves precise cutting of SWNTs, (B) opening of a SWNT yields carboxylic acid-functionalized point contacts separated by ~2 nm, and (C) AFM image of the SWNT gap with (inset) height profile of an isolated tube. The diameter of the SWNT is estimated to be 1.6 nm.

diamines and a coupling reagent (Figure 3A,B).[28,30,31] All the measurements described below were measured in ambient conditions. Some of the devices that were open circuits after cutting show a finite conductance after this coupling. Measurements on devices before cutting, when cut, and after reconnection are shown in Figure 3C,D. The background current for the device after cutting was at the noise level of the measurement in the picoamp range. The black curves show the source−drain current (I) plotted against the gate voltage (V_G) at constant S−D bias voltage (V_{SD} = 50 mV). The device in Figure 3C before cutting shows metallic behavior, and that in Figure 3D shows p-type semiconducting behavior. The red traces, taken after the oxidative cutting, show no conductance (down to the noise limit of the measurement, ≤2.0 pA). The green traces show the devices after reconnection. The rejoined devices recovered their original (i.e., metallic or semiconducting) behavior at reduced values of I (the gate modulates the nanotube conductance more strongly than that of the molecules).

Examples of bridges that have been incorporated into SWNT electrodes are shown in Figure 3B. The cruciform π-systems **1**[32] and the longer oligothiophenylene **2**[26] have a path of through-conjugation for current flow, as well as side chains ("R" in the figure) that not only make the molecules highly soluble but also provide them with considerable width. Given the volume occupied by **1**, **2**, and **3**, it is difficult to bridge the gap with more than a few molecules. The amidation reaction also allows for calibration of the etching process. For example, the yield for connection of **1**, as well as that of molecules of length similar to **1**, is ~10%. Under identical conditions, longer molecules **2** and **3** give lower yields in the connection reaction (~5%). The amide junctions avoid some serious drawbacks of the chemistry of thiols on gold: oxidative oligomerization of dithiols, stochastic switching,[4] and lateral surface mobility of metal grains.[33]

The difference between the current in a tube before it is cut and after it is cut and reconnected by a molecule allows us to estimate the conductance of the bridging molecule. For example, the molecular conductance of **1** in the metallic device shown in Figure 3C is calculated to be 6.4×10^{-3} e^2/h. One factor that hampers the extraction of more quantitative information is the device-to-device variation for any given molecule. Variations in the molecular conformation, the possibility of multiple molecular bridges, and the lack of atomic-level precision in the cutting are ongoing challenges.

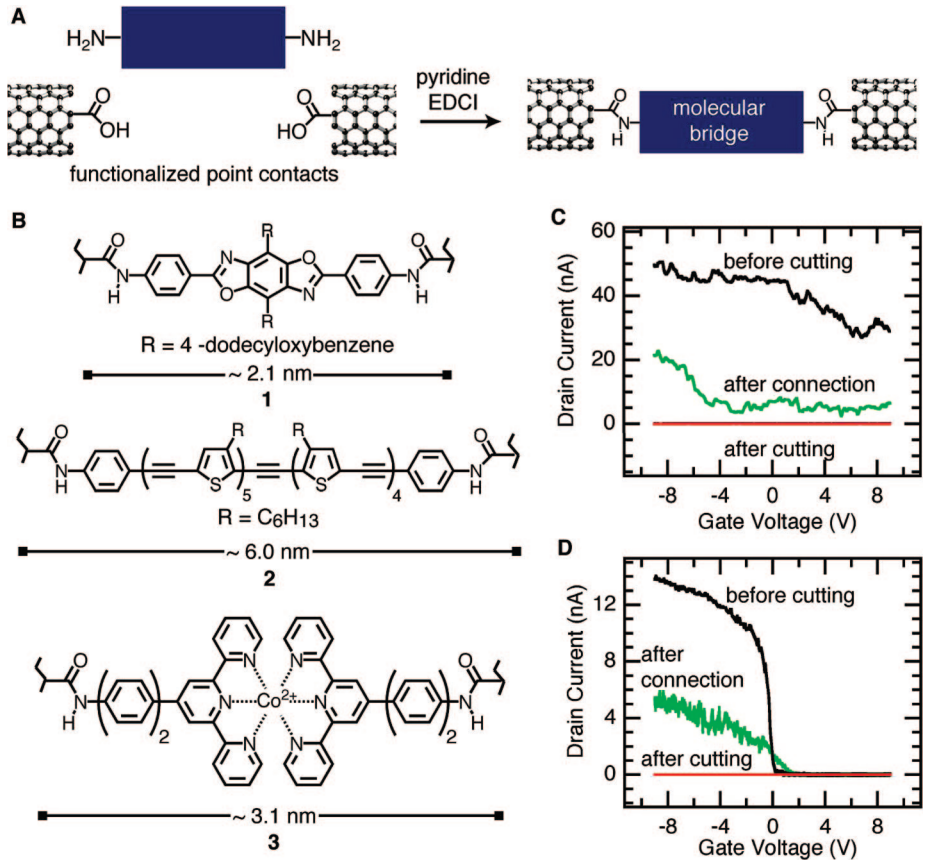

FIGURE 3. (A) Amine bridge joins the gap in SWNT, (B) examples of molecular bridges (**1**−**3**) spanning cut nanotubes, (C) metallic nanotube electrodes connected with **1**, and (D) semiconducting nanotubes electrodes connected with **1**.

Functional Nanoscale Devices: pH Sensing, Metal-Ion Recognition, And Photogated Switching

The amidation is simple and quite general, and the contacts provided by amide-linked molecular bridges are robust; this allows the electrical properties of a wide variety of molecules to be tested. One advantageous consequence is that we are able to install functionality into the devices that allows them to be sensitive to environmental changes. Here we detail molecular devices that are sensitive to pH, metal ions, and light.[26,34]

The electrical resistance of oligoanilines is sensitive to pH in both bulk and molecular-scale devices. We synthesized amine-terminated oligoanilines of a defined length and assayed their conductivities in SWNT devices. The response to pH for the semiconducting device bearing the oligoaniline diamine **4** is shown in Figure 4. The oxidized, emeraldine, form of the oligoaniline **4b** is pH sensitive, the protonated form **4a** being more conductive.[35] A series of protonations (pH = 3) and deprotonations (pH = 11) were performed, and molecular conductance was observed to change by nearly an order of magnitude, from $\sim 5.2 \times 10^{-4}$ e^2/h at low pH to $\sim 5.0 \times 10^{-3}$ e^2/h at high pH over many switching cycles. We attribute the decay in the current in the devices to reorganization and degradation of the junction. When the same experiment is performed on devices connected with **2**, which lacks basic nitrogens and thus should not switch with pH, only a slight pH dependence is seen. It is noteworthy that the change is in the opposite direction from the device connected with the pH- and redox-active oligoaniline **4**. This nanodevice provides a local monitor for pH based on one (or, at most, a few) molecules.

SWNTs joined by molecule **3** (Figure 3) provide a starting point for the fabrication of devices that recognize metal ions (Figure 5). The acid-functionalized ends of cut nanotubes are coupled with terpyridine-containing amines to generate device **5**, which shows conductance at the noise limit of our measurement (red curve on Figure 5B). When the terpyridine ends are ligated with Co(II) ion to form device **6**, the current is partially restored (green curve). This indicates the utility of this method in the construction of multiple-component molecular devices: a single component, the terpyridine, is not sufficient; a second component, the metal ion, is required for a complete circuit. This provides a potentially valuable method

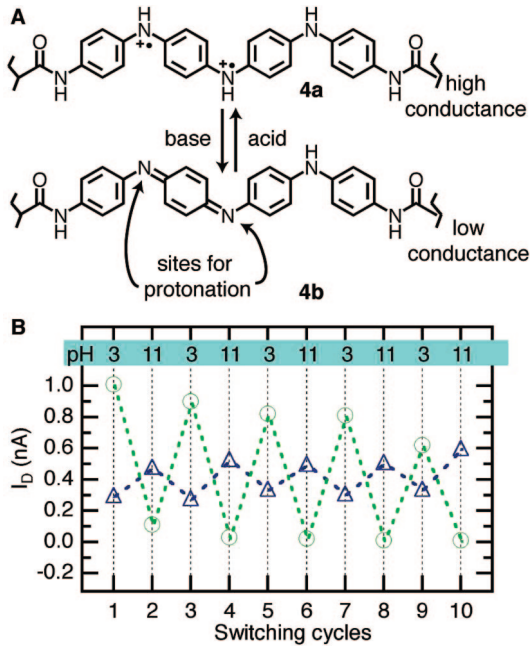

FIGURE 4. (A) Oligoaniline **4** provides a redox- and pH-sensitive molecular bridge. Protonation and deprotonation give rise to high- (**4a**) and low-conductance (**4b**) forms. (B) Green circles show the ON-state resistance for **4** when alternately immersed in solutions of low and high pH. The blue triangles show small changes in ON-state resistance for **2** when alternately immersed in solutions of low and high pH.

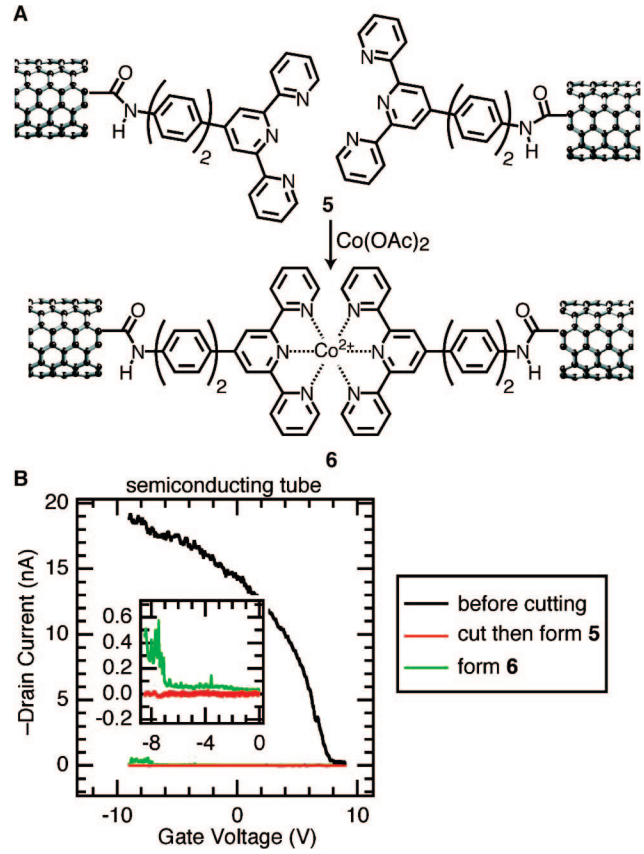

FIGURE 5. (A) Terpyridylamine-functionalized SWNT ends incorporate Co^{2+} ions completing the circuit, and (B) drain current in the device as a function of the gate voltage (V_g).

for the recognition of individual metal ions. This method would only be limited by diffusion of the analyte to the receptor and the association constant between the metal ion and the ligand.

We have also made photodetective molecular devices by bridging the cut in SWNT electrodes with light-sensitive molecular solder.[34] Diarylethenes switch between open (nonconjugated) and closed (conjugated) states[36] and have been installed into single molecular devices with gold contacts.[37,38] The thiophene-based device **7** can be switched from an insulating open form to the conductive closed form but not back again, while the pyrrole-based device **8** does cycle between the open and closed states (Figure 6).

In solution, the diamines that form **7** and **8** photocyclize with UV light (365 nm), and photoreversion occurs with visible light (>500 nm). As expected, when the open **7** device (made with either metallic or semiconducting cut SWNTs) is irradiated with a low-intensity (23 W) UV source (365 nm), there is a 25-fold increase in conductance. We attribute this to the photoclosure of the diarylethene (giving closed **7**) that opens a conjugation pathway between the two SWNT electrodes. When the light is extinguished, the current through the device remains at the higher level for several weeks. Closed **7** is unable to revert back to the open state photochemically.[39]

The pyrrole-based molecular switch, **8**, closes photochemically and reverts to its open state thermally. This supports the hypothesis that it was the excited-state of closed **7** that was responsible for its inability to switch.[40] When a cut SWNT is reconnected with open **8** diamine, the source−drain current is very low (Figure 6C). With UV irradiation, the bridge cyclizes, and the current increases by more than 5 orders of magnitude (Figure 6D). The low-conductance state is restored when the device is kept at room temperature, and the on/off cycle can be toggled many times, although the magnitude of the difference becomes less. The high conductance of closed **8** may be a consequence of multiple bridges in the SWNT gap, because the diameter of the tube can accommodate as many as eight molecular bridges. UV-pulse experiments support the notion of several molecular bridges; there is an observed increase in conductance after each pulse.[34]

The ability to functionalize the ends of cut nanotubes has led to a variety of functional nanoscale devices. SWNT-based sensors for pH changes, metal ions, and light have been assembled and studied. We describe multicomponent single-molecule electronic devices discussed in the next section.

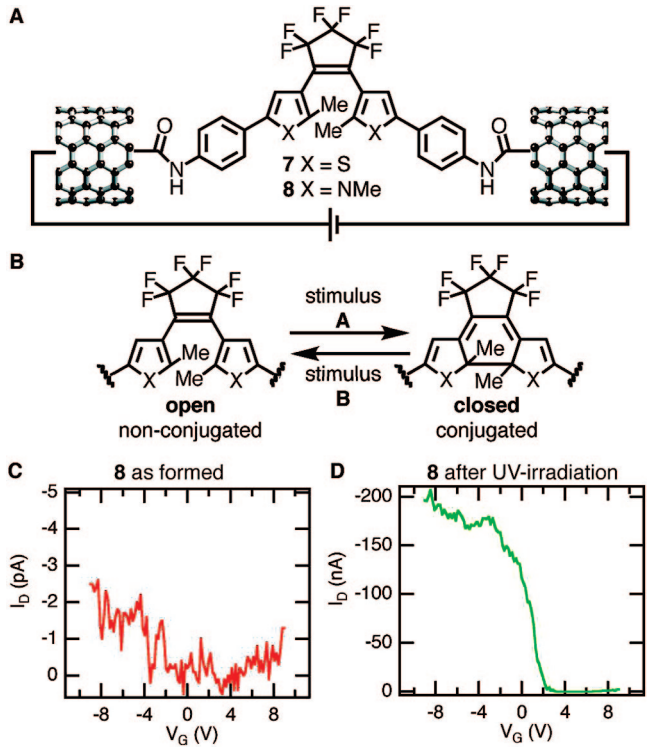

FIGURE 6. (A) Photoswitchable molecular bridges between the ends of individual SWNT electrodes, (B) bridges switch between nonconjugated and conjugated structures, (C) individual semiconducting SWNT bridged with open **8**, and (D) device after UV-irradiation to form closed **8**. This is the same device before UV-irradiation (open **8**).

Single-Molecule Devices as Scaffolding for Studying Individual Protein−Ligand Interactions

We adapted this method to form complex, multicomponent, selectively reactive nanostructures.[41,42] A cut SWNT is bridged with a molecule that is functionalized such that it can be derivatized with a second reagent, a probe molecule. The probe then binds to a third molecule, a complementary binder, to form a noncovalent complex. Each step of assembly can be monitored electrically. One key advantage of this approach to molecular sensing is the ability to form a well-defined linkage between a molecular wire and a probe molecule. Furthermore, because it is constructed from a single molecule, each device has the capacity to monitor individual binding events.[43] This methodology demonstrates an attractive connection between electrical conduction and biology.[24,43−50]

Using the approach outlined above, we have electrically detected oxime formation on the molecular bridge and subsequently detected the noncovalent binding between ligand (biotin) and protein (streptavidin). To do this, cut SWNTs, prepared as described above, are reconnected with the diaminofluorenone (Figure 7A), and the ketone moiety is used as a chemoselective binding site via the formation of an oxime.[51] The fluorenone device **9** is converted to the corresponding oxime-based device **10** by treating it with the alkoxyamine-modified biotin derivative in solution (Figure 7B).

The electrical properties of these devices were characterized by monitoring the current as a function of the voltage applied to the silicon back gate (Figure 7C). The semiconducting device behaves like a p-type transistor, and two of its characteristics change upon reaction: the ON-state resistance and the threshold gate voltage, V_{TH}. The ON-state resistance of the ketone device **9** is higher than that of the oxime device **10** (2.6 vs 2.2 MΩ),[18,19] and V_{TH} in **9** is higher than that in **10** (3.3 vs 2.5 V). The functionalized device **10** is then placed in a solution of streptavidin, a protein known to form a high-affinity complex with biotin. The complex device **11** shows a drastic reduction in ON-state resistance from 2.2 to 1.1 MΩ upon association with streptavidin. This large change in resistance arises from a localized, individual probe molecule wired into the circuit, which makes this system a unique, multicomponent, molecular-scale sensor. The origin of this difference is not well-understood but could arise from ionizable groups of the protein being placed near the molecular bridge.[41]

The programmed information of the biotin/streptavidin binding can be used as a tool to construct even more complex heterostructures. For example, nanoparticles coated with streptavidin are used to localize a Au nanoparticle (Figure 8). There is a decrease in the ON-state resistance and a negative shift in V_{TH}.

Conductivity of a DNA Duplex Bridging a SWNT Gap: DNA Hybridization Sensor

The method of constructing multicomponent conducting devices has been applied to measure the conductivity of a DNA duplex.[42] Numerous charge transport measurements on DNA strands bridging two electrodes have been carried out,[52−55] yielding a remarkably wide range of resistance values ($1-10^7$ MΩ). In all of the DNA conductivity measurements carried out so far, either the integrity of the DNA is not well established, the connections to the duplex are not well defined, or the measurement is not definitively of a single DNA duplex. Therefore, the integration of DNA strands into SWNT electrodes allows the first measurements of electrical properties of a single DNA duplex in its native conformation (*vide infra*).

Two different device conductivities are explored (Figure 9). In one case, the 5′ ends of a DNA duplex are modified with amines, which are then linked to the ends of a cut SWNT (Fig-

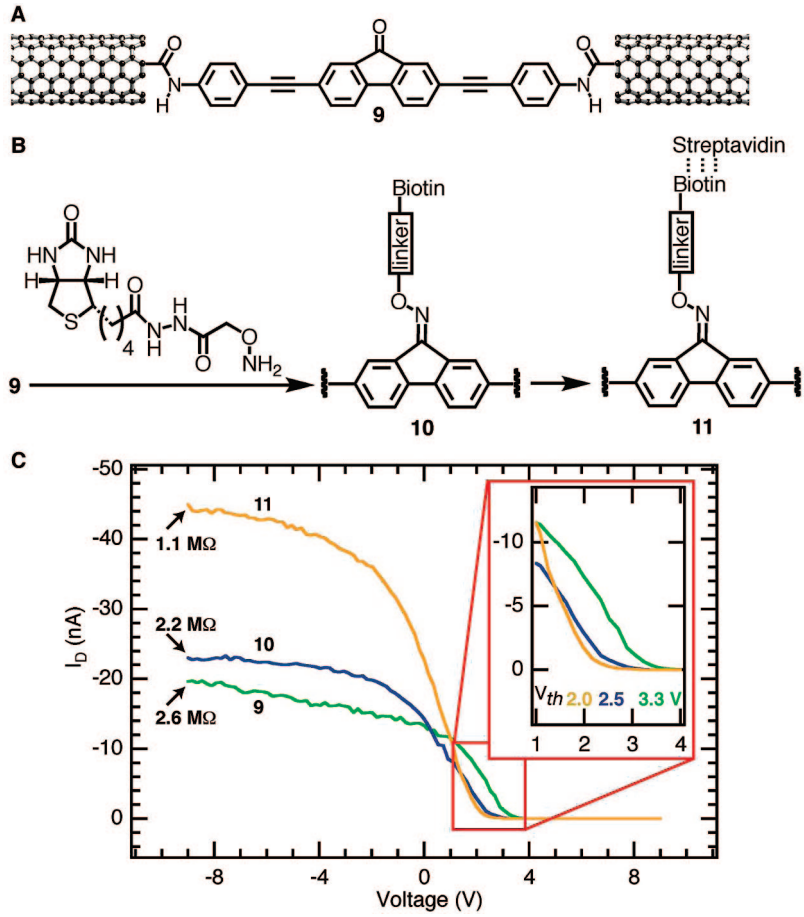

FIGURE 7. (A) Bridging the gap in a cut SWNT with a diamino-substituted fluorenone to form the single-molecule device **9**, (B) reaction sequence where the fluorenone is condensed with an alkoxyamine-derivatized biotin to form the oxime **10** on the molecular bridge, which is then able to bind streptavidin to form the noncovalent complex **11**, and (C) current−voltage characteristics for each step of the reaction sequence.

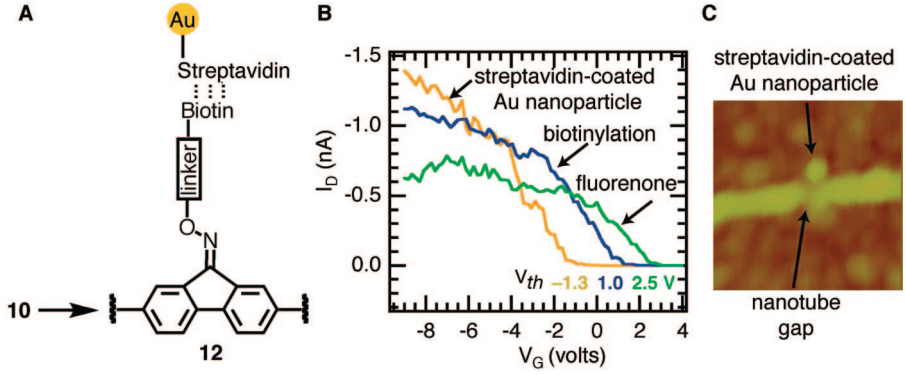

FIGURE 8. (A) Biotin-tethered device **12** binding to a streptavidin-coated ~5 nm gold nanoparticle, (B) current−voltage characteristics for each step of the reaction sequence, and (C) AFM image of a gold nanoparticle located at the molecular junction.

ure 9A) in such a way that each end of the two strands is bound to an electrode. In another case, both the 3′ and the 5′ ends of a single DNA strand are amine-functionalized, and a single strand is bound between SWNT ends (Figure 9B), which allows the measurement of electrical properties of complementary and mismatched strands. The representative *I*−*V* curves for both types of devices are shown in Figure 9. The devices were measured in ambient conditions. Before cutting (black curves), the device in Figure 9A is a p-type semiconductor, while that in Figure 9B is a metallic device. After cutting and initial treatment of the gap with coupling agents (red curves), the devices show no measurable current. The green curves illustrate the conductance after the two devices are reconnected with amine-modified DNA strands. In both cases,

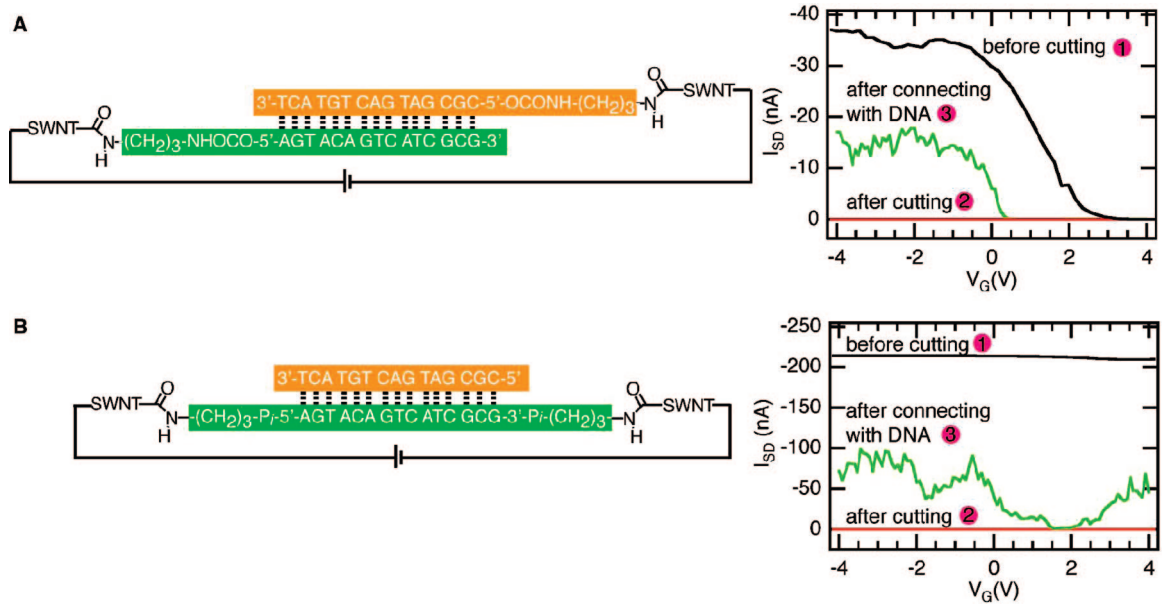

FIGURE 9. Source−drain current vs V_G at a constant source−drain voltage (50 mV) for (A) semiconducting SWNT device with DNA sequence connection and (B) metallic SWNT device with DNA sequence connection.

the reconnected carbon nanotube devices recover their original p-type semiconducting or metallic properties. These measurements place the resistance of well-matched DNA duplexes with ~6 nm length in the range of 0.1−5 MΩ. For comparison, highly oriented pyrolytic graphite (HOPG) with similar dimensions should also be ~1 MΩ.[42]

In a different experiment, devices with mismatched DNA are studied (Figure 10), because DNA-promoted charge transport is found to be exquisitely sensitive to the integrity of the base pair stack.[56,57] A device reconnected with a well-matched (WM) DNA duplex is dehybridized and subsequently rehybridized with two different strands with a mismatch nucleotide, to generate CA and GT mismatches (Figure 10A). Rehybridization with a strand generating a CA mismatch reduces the current significantly and yields an increase in the ON-state resistance of nearly 300-fold from 0.5 to 155 MΩ (Figure 10C). Replacing the CA mismatch with a GT mismatch does not change the device characteristics. The original ON-state resistance and current levels can be recovered by replacing the GT mismatch with the original WM sequence.

The integrity of the DNA duplex is necessary for its conductivity. This is confirmed by an experiment in which a restriction enzyme *Alu* I is used to cut the DNA, eliminating the conductive path. Since the enzyme only acts on DNA in its native conformation, this shows that the DNA duplex is intact under the experimental conditions.

Chemoresponsive Monolayer Transistors

Devices made by cutting and rejoining single-walled carbon nanotubes are not limited to the measurement of the conductivity across a single small molecule. As shown in the previous example using DNA duplexes, the conductance is maintained when two appropriate molecules (in that case, two complementary single strands of DNA) are held together via hydrogen bonding. This method can also measure the current across a set of molecules that self-assemble between two ends of a cut SWNT. Monolayers of polycyclic aromatic hydrocarbons assemble in the gap to complete the transistor structure.[58] These oligomolecular transistors show large current modulation and high gate efficiency.

The devices are formed through self-assembly of organic semiconductors on the oxide surface of a silicon wafer.[59,60] Contorted hexabenzocoronene (HBC) (Figure 11) is used here because compound **13A**, which is surrounded by four alkyl groups, self-organizes into molecular stacks with exceptional semiconducting properties.[61] The molecules are functionalized (Figure 11A) so that they both assemble laterally and covalently attach themselves to the substrate (Figure 11B,C). The coverage on quartz windows is estimated to be ~0.7 molecules in a 1 nm × 1 nm square for both **13B** and **13C**. The monolayers are π-stacked as confirmed by IR, UV−vis, surface X-ray scattering, and photoluminescence.

When the SWNT point contacts detailed above are used as the source and drain electrodes, transistors that have high gate efficiency and large ON/OFF ratios can be made from monolayers of **13B** and **13C**. The electrical properties of these monolayer transistors are responsive to electron acceptors such as tetracyanoquinodimethane (TCNQ) because the active channel of the devices is exposed and available for recogni-

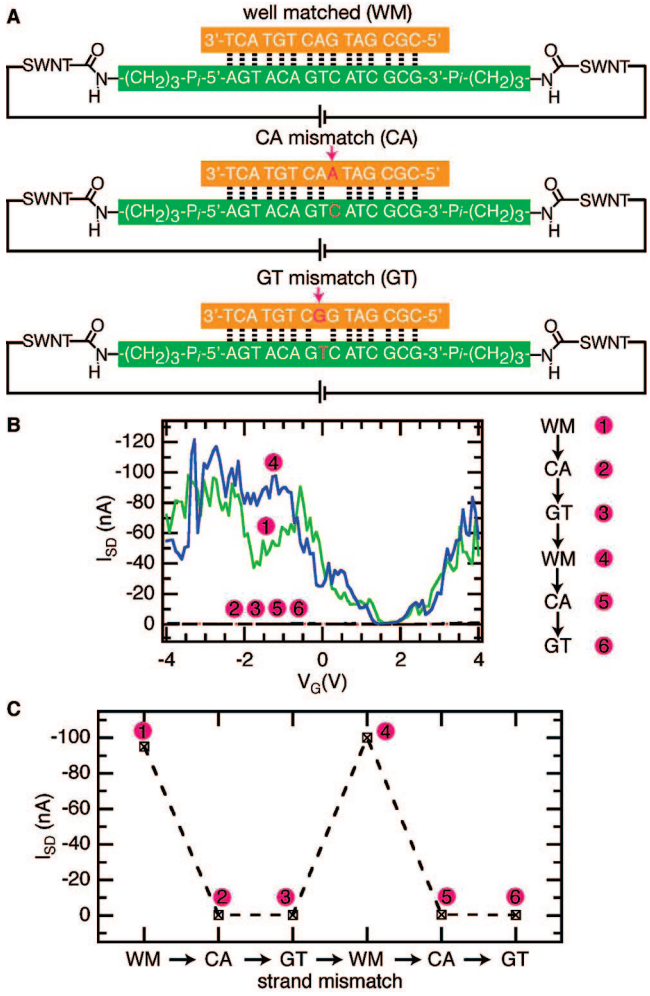

FIGURE 10. (A) Replacing well-matched (WM) duplexes with CA and GT mismatches. (B) Source−drain current versus V_G of a SWNT device taken through the sequence 1 through 6. The current levels for curves 2, 3, 5, and 6 are ~300 times lower. (C) Source−drain current at $V_G = -3$ V at a constant source−drain voltage (−50 mV) for the sequence 1 through 6.

tion. Given the affinity of the electron acceptor TCNQ for the molecules such as coronene,[62] it likely acts as a dopant for the stacks by accepting π-electrons through charge transfer between the electron-deficient TCNQ and the electron-rich HBC. These chemoresponsive devices have utility as ultrasensitive devices for environmental and chemical sensing.

Summary

Cutting single-walled carbon nanotubes and rejoining the ends with conductive organic molecules provides a new generation of nanoscale devices. The ability to perform electrical measurements on truly single-molecule devices allows virtually unlimited possibilities to study the electronic properties of organic molecules and biological systems. Progress in this field has been remarkable. Starting with simple connections of nanotubes by small organic molecules, research has expanded

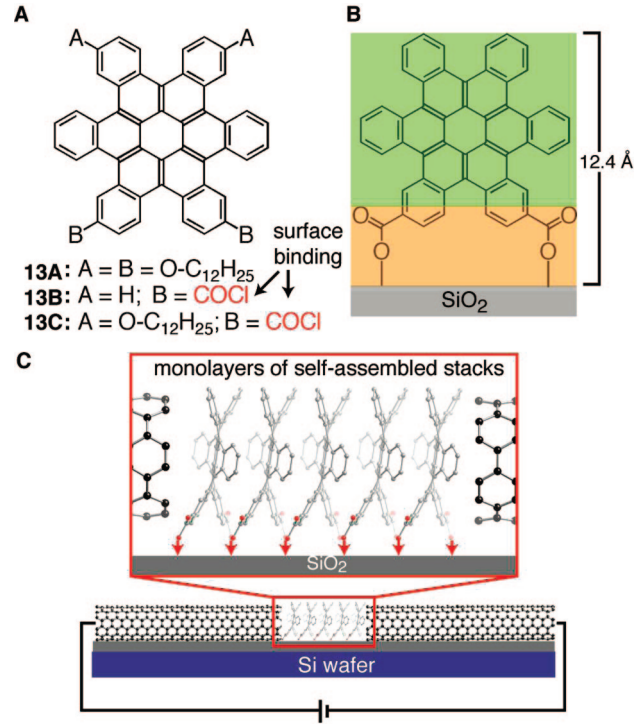

FIGURE 11. (A) HBC molecules. Compound **13A** assembles to 1D stacks; compounds **13B** and **13C** bind to silicon oxide via the acid chloride moieties. (B) Model with three layers color-coded to show relative thickness. (C) Monolayers of self-assembled stacks being probed with SWNT electrodes.

to include molecules with various functionalities. This gave such functional devices as pH, redox, and ion sensors and reversible photogated switches. Furthermore, single-molecule devices have given rise to multicomponent functional assemblies, geared to study important interactions in biology, materials science, and organic chemistry through precisely programmed chemical reactions and molecular recognition. This work is an example of how the ever-reducing dimensions of device fabrication can connect electrical conductivity with seemingly disparate disciplines.

We are grateful to the numerous co-workers and colleagues that contributed to this work. We acknowledge the Nanoscale Science and Engineering Initiative of the NSF under Award Number CHE-0641523 and by the New York State Office of Science, Technology, and Academic Research (NYSTAR); the Chemical Sciences, Geosciences and Biosciences Division, Office of Basic Energy Sciences, US DOE (Grant No. DE-FG02-01ER15264); the NSF NIRT Award (Grant ECCS-0707748); and the MRSEC Program of the National Science Foundation under Award Number DMR-0213574 and by the New York State Office of Science, Technology and Academic Research (NYSTAR) for financial support for M.L.S.

BIOGRAPHICAL INFORMATION

Alina Feldman was born in Kharkov, Ukraine, and moved to the United States in 1996. She completed her undergraduate studies at MIT working with Stephen J. Lippard and received her Ph. D. under the supervision of K. Barry Sharpless at the Scripps Research Institute in 2006. Alina is currently a postdoctoral researcher at Columbia University with Colin Nuckolls.

Mike Steigerwald was born in Michigan in 1956. He did both his undergraduate and graduate training at Caltech, working with Dave Evans, Bill Goddard, and Bob Grubbs. After a postdoctoral position with Marty Semmelhack at Princeton, he joined Bell Laboratories where he worked in solid-state chemistry. He has been at Columbia since 2002.

Xuefeng Guo was born in Luzhou, Sichuan Province, in 1975. He received his Ph.D. in 2004 from the Institute of Chemistry, Chinese Academy of Science, Beijing, under the guidance of Daoben Zhu and Deqing Zhang. From 2004 to 2007, he was a postdoctoral scientist at Columbia University with Colin Nuckolls and Philip Kim. He joined the faculty at Peking University in 2008. His research focuses on the design, fabrication, and optoelectronic properties of nanometer/molecular devices.

Colin Nuckolls was born at Lakenheath RAF in Great Britain in 1970. He completed his undergraduate studies at the University of Texas at Austin studying with Marye Anne Fox and then received his Ph. D. in 1998 from Columbia University with Thomas Katz. He was an NIH postdoctoral fellow with Julius Rebek, Jr., at the Scripps Research Institute. He joined the faculty at Columbia University in 2000, and in 2006, he was promoted to the rank of Professor.

FOOTNOTES

*To whom correspondence should be addressed. E-mail addresses: guoxf@pku.edu.cn; cn37@columbia.edu.

REFERENCES

1 Tour, J. M. Molecular electronics. Synthesis and testing of components. *Acc. Chem. Res.* **2000**, *33*, 791–804.

2 Flood, A. H.; Stoddardt, J. F.; Steuerman, D. W.; Heath, J. R. Whence molecular electronics? *Science* **2004**, *306*, 2055–2056.

3 Heath, J. R.; Ratner, M. A. Molecular electronics. *Phys. Today* **2003**, *56*, 43–49.

4 Ramachandran, G. K.; Hopson, T. J.; Rawlett, A. M.; Nagahara, L. A.; Primak, A.; Lindsay, S. M. A bond-fluctuation mechanism for stochastic switching in wired molecules. *Science* **2003**, *300*, 1413–1416.

5 Metzger, R. M. Unimolecular rectifiers and proposed unimolecular amplifier. *Ann. N.Y. Acad. Sci.* **2003**, *1006*, 252–276.

6 Nitzan, A.; Ratner Mark, A. Electron transport in molecular wire junctions. *Science* **2003**, *300*, 1384–1389.

7 Salomon, A.; Cahen, D.; Lindsay, S.; Tomfohr, J.; Engelkes, V. B.; Frisbie, C. D. Comparison of electronic transport measurements on organic molecules. *Adv. Mater.* **2003**, *15*, 1881–1890.

8 Reed, M. A.; Zhou, C.; Muller, C. J.; Burgin, T. P.; Tour, J. M. Conductance of a molecular junction. *Science* **1997**, *278*, 252–254.

9 Liang, W.; Bockrath, M.; Bozovic, D.; Hafner, J. H.; Tinkham, M.; Park, H. Fabry–Perot interference in a nanotube electron waveguide. *Nature* **2001**, *411*, 665–9.

10 Cui, X. D.; Primak, A.; Zarate, X.; Tomfohr, J.; Sankey, O. F.; Moore, A. L.; Moore, T. A.; Gust, D.; Harris, G.; Lindsay, S. M. Reproducible measurement of single-molecule conductivity. *Science* **2001**, *294*, 571–574.

11 Xu, B.; Tao, N. J. Measurement of single-molecule resistance by repeated formation of molecular junctions. *Science* **2003**, *301*, 1221–1223.

12 Venkataraman, L.; Klare, J. E.; Nuckolls, C.; Hybertsen, M. S.; Steigerwald, M. L. Dependence of single-molecule junction conductance on molecular conformation. *Nature* **2006**, *442*, 904–907.

13 Cui, X. D.; Primak, A.; Zarate, X.; Tomfohr, J.; Sankey, O. F.; Moore, A. L.; Moore, T. A.; Gust, D.; Nagahara, L. A.; Lindsay, S. M. Changes in the electronic properties of a molecule when it is wired into a circuit. *J. Phys. Chem. B* **2002**, *106*, 8609–8614.

14 Mayor, M.; Weber, H. B. Statistical analysis of single-molecule junctions. *Angew. Chem., Int. Ed.* **2004**, *43*, 2882–2884.

15 Zhitenev, N. B.; Erbe, A.; Bao, Z. Single- and multigrain nanojunctions with a self-assembled monolayer of conjugated molecules. *Phys. Rev. Lett.* **2004**, *92*, 186805/1–186805/4.

16 Zhitenev, N. B.; Meng, H.; Bao, Z. Conductance of small molecular junctions. *Phys. Rev. Lett.* **2002**, *88*, 226801/1–226801/4.

17 Takata, T.; Kim, Y. H.; Oae, S. Reaction of organic sulfur compounds with superoxide anion: Oxidation of disulfides, thiolsulfinates and thiolsulfonates to their sulfinic and sulfonic acids. *Tet. Lett.* **1979**, 821–824.

18 Venkataraman, L.; Park, Y. S.; Whalley, A. C.; Nuckolls, C.; Hybertsen, M. S.; Steigerwald, M. L. Electronics and chemistry: Varying single-molecule junction conductance using chemical substituents. *Nano Lett.* **2007**, *7*, 502–506.

19 Venkataraman, L.; Klare, J. E.; Tam, I. W.; Nuckolls, C.; Hybertsen, M. S.; Steigerwald, M. L. Single-molecule circuits with well-defined molecular conductance. *Nano Lett.* **2006**, *6*, 458–462.

20 Iijima, S. Helical microtubules of graphitic carbon. *Nature* **1991**, *354*, 56–58.

21 Robertson, J. Growth of nanotubes for electronics. *Mater. Today* **2007**, *10*, 36–43.

22 Thompson, S. E.; Parthasarathy, S. Moore's law: The future of si microelectronics. *Mater. Today* **2006**, *9*, 20–25.

23 Avouris, P. Molecular electronics with carbon nanotubes. *Acc. Chem. Res.* **2002**, *35*, 1026–1034.

24 Dai, H. Carbon nanotubes: Synthesis, integration, and properties. *Acc. Chem. Res.* **2002**, *35*, 1035–1044.

25 Tans, S. J.; Verschueren, A. R. M.; Dekker, C. Room-temperature transistor based on a single carbon nanotube. *Nature* **1998**, *393*, 49–52.

26 Guo, X.; Small, J. P.; Klare, J. E.; Wang, Y.; Purewal, M. S.; Tam, I. W.; Hong, B. H.; Caldwell, R.; Huang, L.; O'Brien, S.; Yan, J.; Breslow, R.; Wind, S. J.; Hone, J.; Kim, P.; Nuckolls, C. Covalently bridging gaps in single-walled carbon nanotubes with conducting molecules. *Science* **2006**, *311*, 356–359.

27 Qi, P.; Javey, A.; Rolandi, M.; Wang, Q.; Yenilmez, E.; Dai, H. Miniature organic transistors with carbon nanotubes as quasi-one-dimensional electrodes. *J. Am. Chem. Soc.* **2004**, *126*, 11774–11775.

28 Niyogi, S.; Hamon, M. A.; Hu, H.; Zhao, B.; Bhowmik, P.; Sen, R.; Itkis, M. E.; Haddon, R. C. Chemistry of single-walled carbon nanotubes. *Acc. Chem. Res.* **2002**, *35*, 1105–1113.

29 Huang, L.; Cui, X.; White, B.; O'Brien, S. P. Long and oriented single-walled carbon nanotubes grown by ethanol chemical vapor deposition. *J. Phys. Chem. B* **2004**, *108*, 16451–16456.

30 Chiu, P.-W.; Kaempgen, M.; Roth, S. Band-structure modulation in carbon nanotube t-junctions. *Phys. Rev. Lett.* **2004**, *92*, 246802/1–246802/4.

31 Artukovic, E.; Kaempgen, M.; Hecht, D. S.; Roth, S.; Gruener, G. Transparent and flexible carbon nanotube transistors. *Nano Lett.* **2005**, *5*, 757–760.

32 Klare, J. E.; Tulevski, G. S.; Nuckolls, C. Chemical reactions with upright monolayers of cruciform p-systems. *Langmuir* **2004**, *20*, 10068–10072.

33 Houck, A. A.; Labaziewicz, J.; Chan, E. K.; Folk, J. A.; Chuang, I. L. Kondo effect in electromigrated gold break junctions effect in electromigrated gold break junctions. *Nano Lett.* **2005**, *5*, 1685–1688.

34 Whalley, A. C.; Steigerwald, M. L.; Guo, X.; Nuckolls, C. Reversible switching in molecular electronic devices. *J. Am. Chem. Soc.* **2007**, *129*, 12590–12591.

35 MacDiarmid, A. G. "Synthetic metals": A novel role for organic polymers (Nobel lecture). *Angew. Chem., Int. Ed.* **2001**, *40*, 2581–2590.

36 Irie, M. Diarylethenes for memories and switches. *Chem. Rev.* **2000**, *100*, 1685–1716.

37 Dulic, D.; van der Molen, S. J.; Kudernac, T.; Jonkman, H. T.; de Jong, J. J. D.; Bowden, T. N.; van Esch, J.; Feringa, B. L.; van Wees, B. J. One-way optoelectronic switching of photochromic molecules on gold. *Phys. Rev. Lett.* **2003**, *91*, 207402/1–207402/4.

38 He, J.; Chen, F.; Liddell, P. A.; Andreasson, J.; Straight, S. D.; Gust, D.; Moore, T. A.; Moore, A. L.; Li, J.; Sankey, O. F.; Lindsay, S. M. Switching of a photochromic molecule on gold electrodes: Single-molecule measurements. *Nanotechnology* **2005**, *16*, 695–702.

39 For the measurements of SWNTs connected with thiophene-based device **7**, please see: Whalley, A. C.; Steigerwald, M. L.; Guo, X.; Nuckolls, C. Reversible switching in molecular electronic devices. *J. Am. Chem. Soc.* **2007**, *129*, 12590–12591.

40 Nakamura, S.; Irie, M. Thermally irreversible photochromic systems. A theoretical study. *J. Org. Chem.* **1988**, *53*, 6136–6138.

41 Guo, X.; Whalley, A.; Klare, J. E.; Huang, L.; O'Brien, S.; Steigerwald, M.; Nuckolls, C. Single-molecule devices as scaffolding for multicomponent nanostructure assembly. *Nano Lett.* **2007**, *7*, 1119–1122.

42 Guo, X.; Gorodetsky, A. A.; Hone, J.; Barton, J. K.; Nuckolls, C. Conductivity of a single DNA duplex bridging a carbon nanotube gap. *Nat. Nanotechnol.* **2008**, *3*, 163–167.

43 Patolsky, F.; Zheng, G.; Hayden, O.; Lakadamyali, M.; Zhuang, X.; Lieber, C. M. Electrical detection of single viruses. *Proc. Natl. Acad. Sci. U.S.A.* **2004**, *101*, 14017–14022.

44 Chen, R. J.; Bangsaruntip, S.; Drouvalakis, K. A.; Kam, N. W. S.; Shim, M.; Li, Y.; Kim, W.; Utz, P. J.; Dai, H. Noncovalent functionalization of carbon nanotubes for highly specific electronic biosensors. *Proc. Natl. Acad. Sci. U.S.A.* **2003**, *100*, 4984–4989.

45 Cui, Y.; Wei, Q.; Park, H.; Lieber, C. M. Nanowire nanosensors for highly sensitive and selective detection of biological and chemical species. *Science* **2001**, *293*, 1289–1292.

46 Fan, R.; Karnik, R.; Yue, M.; Li, D.; Majumdar, A.; Yang, P. DNA translocation in inorganic nanotubes. *Nano Lett.* **2005**, *5*, 1633–1637.

47 Li, Y.; Qian, F.; Xiang, J.; Lieber, C. M. Nanowire electronic and optoelectronic devices. *Mater. Today* **2006**, *9*, 18–27.

48 Patolsky, F.; Timko, B. P.; Yu, G.; Fang, Y.; Greytak, A. B.; Zheng, G.; Lieber, C. M. Detection, stimulation, and inhibition of neuronal signals with high-density nanowire transistor arrays. *Science* **2006**, *313*, 1100–1104.

49 Patolsky, F.; Zheng, G.; Lieber, C. M. Nanowire-based biosensors. *Anal. Chem.* **2006**, *78*, 4260–4269.

50 Zheng, G.; Patolsky, F.; Cui, Y.; Wang, W. U.; Lieber, C. M. Multiplexed electrical detection of cancer markers with nanowire sensor arrays. *Nat. Biotechnol.* **2005**, *23*, 1294–1301.

51 Freeman, J. P. Less familiar reactions of oximes. *Chem. Rev.* **1973**, *73*, 283–292.

52 Fink, H.-W.; Schonenberger, C. Electrical conduction through DNA molecules. *Nature* **1999**, *398*, 407–410.

53 Porath, D.; Bezryadin, A.; de Vries, S.; Dekker, C. Direct measurement of electrical transport through DNA molecules. *Nature* **2000**, *403*, 635–638.

54 van Zalinge, H.; Schiffrin, D. J.; Bates, A. D.; Starikov, E. B.; Wenzel, W.; Nichols, R. J. Variable-temperature measurements of the single-molecule conductance of double-stranded DNA. *Angew. Chem., Int. Ed.* **2006**, *45*, 5499–5502.

55 Hihath, J.; Xu, B.; Zhang, P.; Tao, N. Study of single-nucleotide polymorphisms by means of electrical conductance measurements. *Proc. Natl. Acad. Sci. U.S.A.* **2005**, *102*, 16979–16983.

56 Kelley, S. O.; Barton, J. K. Electron transfer between bases in double helical DNA. *Science* **1999**, *283*, 375–381.

57 Kelley, S. O.; Holmlin, R. E.; Stemp, E. D. A.; Barton, J. K. Photoinduced electron transfer in ethidium-modified DNA duplexes: Dependence on distance and base stacking. *J. Am. Chem. Soc.* **1997**, *119*, 9861–9870.

58 Guo, X.; Myers, M.; Xiao, S.; Lefenfeld, M.; Steiner, R.; Tulevski, G. S.; Tang, J.; Baumert, J.; Leibfarth, F.; Yardley, J. T.; Steigerwald, M. L.; Kim, P.; Nuckolls, C. Chemoresponsive monolayer transistors. *Proc. Natl. Acad. Sci. U.S.A.* **2006**, *103*, 11452–11456.

59 Kagan, C. R.; Afzali, A.; Martel, R.; Gignac, L. M.; Solomon, P. M.; Schrott, A. G.; Ek, B. Evaluations and considerations for self-assembled monolayer field-effect transistors. *Nano Lett.* **2003**, *3*, 119–124.

60 Tulevski, G. S.; Miao, Q.; Fukuto, M.; Abram, R.; Ocko, B.; Pindak, R.; Steigerwald, M. L.; Kagan, C. R.; Nuckolls, C. Attaching organic semiconductors to gate oxides: In situ assembly of monolayer field effect transistors. *J. Am. Chem. Soc.* **2004**, *126*, 15048–15050.

61 Xiao, S.; Myers, M.; Miao, Q.; Sanaur, S.; Pang, K.; Steigerwald, M. L.; Nuckolls, C. Molecular wires from contorted aromatic compounds. *Angew. Chem., Int. Ed.* **2005**, *44*, 7390–7394.

62 Chi, X.; Besnard, C.; Thorsmolle, V. K.; Butko, V. Y.; Taylor, A. J.; Siegrist, T.; Ramirez, A. P. Structure and transport properties of the charge-transfer salt coronene-tcnq. *Chem. Mater.* **2004**, *16*, 5751–5755.